Chinese Chemical Letters 32 (2021) 2369–2379

Contents lists available at ScienceDirect

Chinese Chemical Letters

journal homepage: www.elsevier.com/locate/cclet

Review

Development of bioorthogonal SERS imaging probe in biological and biomedical applications

Chonggui Qiu[1], Ziyi Cheng[1], Chuanzhu Lv*, Rui Wang*, Fabiao Yu*

The First Affiliated Hospital of Hainan Medical University, Key Laboratory of Emergency and Trauma, Ministry of Education, Key Laboratory of Hainan Trauma and Disaster Rescue, Institute of Functional Materials and Molecular Imaging, College of Pharmacy, College of Emergency and Trauma, Hainan Medical University, Haikou 571199, China

ARTICLE INFO

Article history:
Received 14 January 2021
Received in revised form 5 March 2021
Accepted 7 March 2021
Available online 9 March 2021

Keywords:
Surface-enhanced Raman scattering (SERS)
Bioorthogonal molecule
Visualization
Disease diagnosis
Therapy

ABSTRACT

Living-cell imaging demands high specificity, sensitivity, and minimal background interference to the targets of interest. However, developing a desirable imaging probe that can possess all the above features is still challenging. The bioorthogonal surface-enhanced Raman scattering (SERS) imaging has been recently emerged through utilizing Raman reporters with characteristic peaks in Raman-silent region of cells (1800–2800 cm^{-1}), which opens a revolutionary avenue for living-cell imaging with multiplexing capability. In this review, we focus on the recent advances in the technology development and the biological and biomedical applications of the living-cell bioorthogonal SERS imaging technique. After introduction of fundamental principles for bioorthogonal tag or label, we present applications for visualization of various intracellular components and environment including proteins, nucleic acids, lipids, pH and hypoxia, even for cancer diagnosis in tissue samples. Then, various bioorthogonal SERS imaging-guided therapy strategies have been discussed such as phototherapy and surgery. In conclusion, this strategy has great potential to be a flexible and robust tool for visualization detection and diseases diagnosis.

1. Introduction

The rapid detection and efficient therapy of diseases are very important for clinical medicine. However, the current methods for rapid detection and early treatment in clinical medicine cannot yet meet the clinical requirement. Therefore, it is an urgent need to develop analytical methods with rapid detection, low background inference and high sensitivity for biological and biomedical applications. In the past decades, the application of surface-enhanced Raman scattering (SERS) in biomedicine and medical transformation has attracted widespread interest from investigation of cellular function to cancer diagnosis and even *in vivo* detection [1]. On rough precious metal surfaces, the inelastic light scattering of molecules can be greatly enhanced (by factors up to 10^{14}-10^{15}). It shows the advantages of special biological detection: (1) high detection sensitivity with excellent detection limit even reaching pmol/L; (2) strong multi-component detection ability; (3) no aqueous solution background signal interference [2,3].

SERS theory has been studied by many scientists, in which two primary theoretical mechanisms have been developed including electromagnetic (EM) enhancement and chemical enhancement (CE). EM enhancement is commonly thought to make major contribution to the Raman signal enhancement [4,5]. When the light irradiates the surface of novel metal nanoparticles (NPs), it will induce collective oscillations from the NPs' surface electrons, which is known as surface plasmon resonance (SPR). When the incident light interacts with the plasmon, the dipolar field can be created with the exciting electric field. The phenomenon of redistribution of the local field induces a great enhancement of EM field at the specific position of the NPs as known as 'hot spot', which induced the enhanced Raman signals of the molecules located at hot spot. The EM enhancement mechanism cannot explain all the SERS phenomenon [6]. Then, CE mechanism has been proposed to explain why the Raman signal is enhanced by one or two orders of magnitude. CE involves the interaction between the adsorbed molecules and noble metal surface, which is mainly described in two ways [7]. The first explanation is that the charge intermediate induced by the interaction of molecules with the surface exhibits higher Raman scattering cross sections than that

* Corresponding authors.
E-mail addresses: lyuchuanzhu@hainmc.edu.cn (C. Lv), wangrui@hainmc.edu.cn (R. Wang), yufabiao@hainmc.edu.cn (F. Yu).
[1] These authors contributed equally to this work.

https://doi.org/10.1016/j.cclet.2021.03.016
1001-8417/

of unadsorbed analytes on the surface [8]. The other description is that the lowest unoccupied molecular orbital (LUMO) and the highest occupied molecular orbital (HOMO) of chemically adsorbed molecules decrease symmetrically with respect to the Fermi level of the metal surface, and the energy required for the transition decreases [9]. Therefore, the charge transfer between the metal surface and the adsorbate can generate Raman excitation photons, which depends on the chemical characteristics of the analyte.

Bioorthogonal reaction is a chemical reaction carried out in a physiological environment but does not interfere with its biological process [10–12]. A common bioorthogonal reaction labeling strategy is usually to perform a bioorthogonal reaction between a biomolecule labeled with a chemical reporter group and bioorthogonal probes carrying a pairing group [11,13,14]. As the most used functional groups in click chemistry, azide and alkyne attract much attention, which have been widely utilized in medicine development, bioimaging and *in vivo* analysis [15,16]. The bioorthogonal reaction labeling strategy has been widely used in proteins, lipids, nucleic acids and glycans. This method enables the chemical reporter group to be metabolized into newly synthesized biomolecules [17,18]. The bioorthogonal reaction labeling strategy is suitable for detecting the dynamic changes of biomolecules in the biological process.

In previous reports, a chemical reporter strategy has been developed to improve the efficiency. The precursors of the modified bioorthogonal functional groups are synthesized by the cell synthesis mechanism to be used for labeling nucleic acids, proteins or glycans. Then, the bioorthogonal functional group is reacted with a fluorescent probe that has been conjugated with a paired bioorthogonal functional group through bioorthogonal chemistry. Up to now, SERS signal detection in organisms is often interfered by the background Raman signals. Inspired by this smart strategy, combing bioorthogonal label with SERS imaging might yield a new live-cell imaging strategy with high sensitivity and specificity, which can directly modify bioorthogonal molecules as Raman reporter molecules [15,19]. The bond vibration of the Raman reporter is in the Raman-silent region (1800–2800 cm^{-1})

Table 1
Summary of recently reported bioorthogonal Raman reporters.

Bioorthogonal Raman reporter	Advantage	Raman peak	Ref.
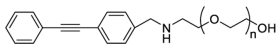	Strong surface plasmon resonance effect	2220 cm^{-1}	[25]
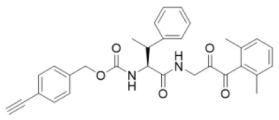	Identifying small molecule binding sites	1958 cm^{-1}	[33]
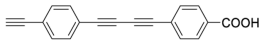	Early cancer phenotype identification.	2205 cm^{-1}	[38]
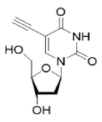	Displaying the nucleus	2119 cm^{-1}	[57]
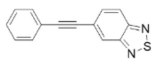	Real-time ratio probe detects CO	2170–2240 cm^{-1}	[64]
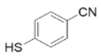	Intracellular ROS detection	2226 cm^{-1}	[66]
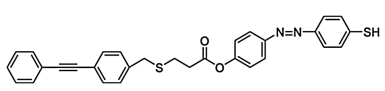	Live cell or tissue imaging in hypoxia	2578 cm^{-1}	[69]
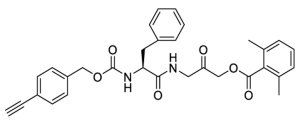	Real-time monitoring of drug absorption	2122 cm^{-1}	[71]
	Monitor dynamic pH changes	2138 cm^{-1}	[75]
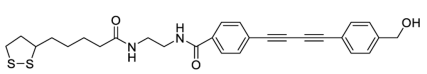	Accurate diagnosis and effective treatment	2205 cm^{-1}	[81]

of the biological sample, and it is hardly disturbed by the Raman signal from the cellular components [10]. This is essential for the rapid detection and early diagnosis of cancer and other diseases [20]. In this review, we will focus on the most recent advances in the development of bioorthogonal SERS strategies. First, we will give brief fundamental principles of bioorthogonal SERS strategies. Next, we will discuss the application in biological analysis and the therapy methods. Finally, we will present the outlook and the future perspectives of this field.

2. Fundamental principles of bioorthogonal SERS

Bioorthogonal SERS probes are usually composed of metal nanoparticle cores, bioorthogonal Raman reporter molecules and biocompatible shells [21]. The bioorthogonal probes can be targeted by modified targeting recognition ligands or surface functionalization. Compared with fluorescent probes, bioorthogonal SERS probes have higher sensitivity and higher multiplexing and quantitative capabilities. In addition, bioorthogonal SERS probes also overcome the spontaneous Raman signal ($1000–1800\ cm^{-1}$) of biological samples and realize spectral biological detection and molecular imaging in the Raman-silent region ($1800–2800\ cm^{-1}$). The molecules naturally present in cells do not have any Raman signal in this region. Therefore, the Raman reporter molecule with Raman signal in this region is specific and not interfered by the background signal of the biological sample. Among the bioorthogonal Raman reporter molecules, the two most popular bioorthogonal chemical reporter molecules, azide and alkynes, can also be used as bioorthogonal Raman reporter molecules, which also include the molecules with functional groups of nitrile and carbon deuterium bond C–D [22,23]. Here, we summarize the bioorthogonal Raman reporters that recently reported as shown in Table 1.

Noble metal nanoparticles including gold (Au) nanoparticles and silver (Ag) nanoparticles have been widely used as substrates in SERS technology. Ag has stronger SPR effect and lower cost than Au, but Ag is more susceptible to environmental factors than Au, which reduces the plasma signal and limits its application. To improve the stability of SERS substrate and reduce the interference of surrounding environment, AgCu@graphene nanoparticles (ACG NPs) were developed and synthesized for Raman imaging where the growing graphene on the AgCu alloy surface can protect the Ag surface (Fig. 1a) [24]. The AgCu alloy NPs were constructed as active substrate, which was protected by directly wrapping multilayer-graphene on the outer layer and then further functionalized with alkyne-polyethylene glycol. The unique signal of the alkyne group provided more accurate cell imaging. ACG NPs exhibited strong SERS enhancement capabilities and resistance against H_2O_2, H_2S or HNO_3. In the subsequent Raman detection and Raman imaging experiments of living cells, it was also found that ACG NPs could accurately locate cells and achieve highly specific Raman imaging [25].

The analysis of biomarkers plays important role in clinical diagnosis and monitoring treatment process [26]. At present, the standard clinical method to detect biomarkers in biological samples is usually through immunohistochemistry (IHC), however, it cannot detect and analyze multiple biomarkers simultaneously. As alternatives, various detection methods have been developed for the analysis of multiple biomarkers including as mass spectrometry (MS), reverse transcription PCR and fluorescence

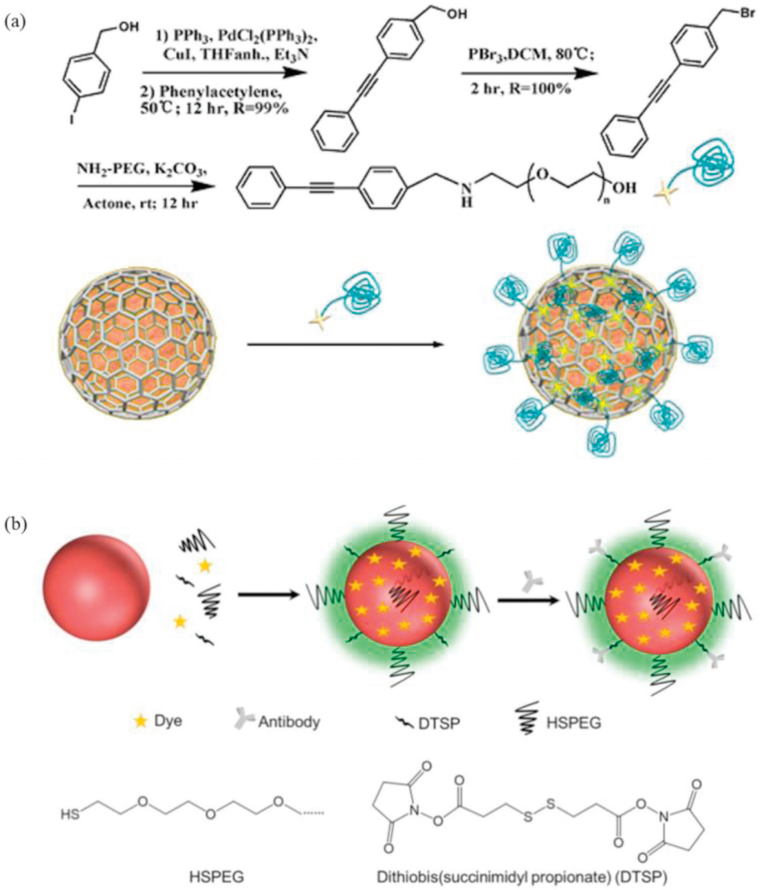

Fig. 1. (a) Preparation of alkyne-PEG-modified ACGs. Copied with permission [25]. Copyright 2014, American Chemical Society; (b) Construction of a background-free SERS tag and the molecular structure of HSPEG and dithiobis. Copied with permission [29]. Copyright 2019, Ivyspring International Publisher.

analysis. Unfortunately, the major methods require destructive preparation of cell or tissue specimens, which leads to the loss of three-dimensional information. The commonly used fluorescence imaging suffers from spectral crosstalk and photobleaching. Therefore, it is highly desirable to develop new techniques for analysis of multiple biomarkers [27,28].

The bioorthogonal SERS tag maybe the possible strategy for the imaging of multiple biomarkers in cancer cells and tissues. A library of bioorthogonal Raman reporters with alkynyl and nitrile groups were designed and synthesized, and then anchored on the surface of AuNPs, which exhibited classic Raman peaks in the Raman-silent region. To obtain multiple targeted SERS nanoprobes, these SERS tags were conjugated with different antibodies against estrogen receptor (ER), progesterone receptor (PR) and epidermal growth factor receptor (EGFR) (Fig. 1b). Multicolor SERS imaging with three different biological targets in human breast cancer tissue could be realized, which aroused widespread interest in early clinical detection [29].

3. SERS-based bioorthogonal analysis

3.1. Protein

Proteins as large biomolecules have complexed three-dimensional structures, performing various vital functions within organisms, including metabolic reactions, immunity, transport and DNA replication [30,31]. Identification of binding sites in protein attracts much attention in chemical biology research [32]. Due to its vital important roles in drug delivery and analysis of protein function, liquid chromatograph-mass spectrometer (LC–MS) has been widely applied to recognize the residue(s) in proteolytic digests; however, the analysis based on LC–MS is often hindered in practical application owing to the complexity of protein digests.

To overcome the limitation, Ando and coworker reported a new strategy based on alkyne-tag Raman screening (ATRaS) for identification of binding sites (Fig. 2a) [33]. In this strategy, the small molecules were labeled with alkyne group and covalently bound to the targeted protein, which was enzymically digested to provide peptide fragments [34]. Two synthetic peptides, propargylglycine or isoleucine, were prepared as models of proteolytic fragments. Upon mixing with 40 nm silver nanoparticles, a strong Raman peak of alkyne was observed at 1958 cm^{-1} in alkyne-labeled peptide sample, while no such peak could be detected in isoleucine sample. The above strong peak could be attributed to chemical enhancement due to charge-transfer between alkyne group and silver nanoparticle. In addition, the addition of trifluoroacetic acid (TFA) induced strong aggregation of silver nanoparticles and peptides, further promoted the uniform distribution on the glass substrate. Thus, SERS text variation in different microwells could be effectively suppressed. With the assistance of line-shaped laser illumination, SERS detection with high reproducibility and sensitivity could be achieved with detection limit of ~100 femtomole.

To investigate the application in practical samples, ATRaS was utilized to recognize the inhibitor-binding site and specificity of cysteine protease cathepsin B (CatB), which involved in cancer progression (Fig. 2b). The specific CatB peptide inhibitor Z-FG-AOMK was screened and selected as the inhibitor model, which contained an acyloxymethyl ketone (AOMK) group selectively interacting with cysteine protease. Then, Z-FG-AOMK was tagged with alkyne to form alkyne-tagged Z-FG-AOMK (Alt-AOMK),

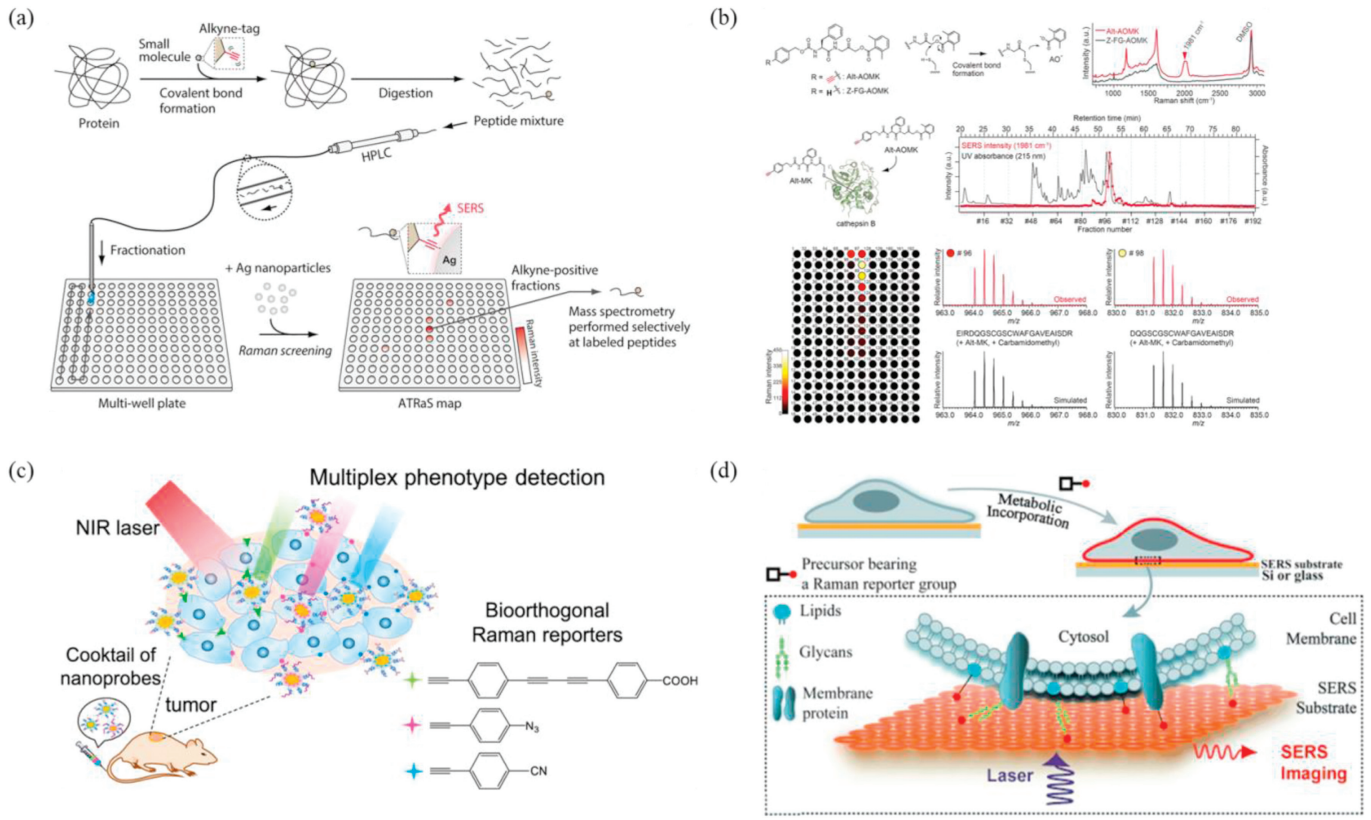

Fig. 2. (a, b) Schematic illustration of Alkyne-Tag Raman Screening (ATRaS) and ATRaS for identification of inhibitor-binding site in cathepsin B (CatB). Copied with permission [33]. Copyright 2016, American Chemical Society; (c) Cocktail of bioorthogonal SERS nanoprobes for simultaneous multiplex cancer phenotype targeting and diagnosis in mice after intravenous injection. Copied with permission [38]. Copyright 2019, American Chemical Society; (d) Schematic illustration of visualizing cell-surface biomolecules by SERS imaging. Copied with permission [41]. Copyright 2014, Wiley Online Library.

retaining the similar inhibitory activity with Z-FG-AOMK due to little effect of alkyne tag on the binding affinity. After labeling CatB with Alt-AOMK, the labeled CatB was digested by trypsin. The peptide mixture was segregated by HPLC, accompanying the reduced cysteine residue with alkyne label of iodoacetamide. Next, the peptide fragments were collected by a glass-bottomed 384-well correlate at 20-sintervas. Upon addition of silver nanoparticles, ATRaS and SERS spectra could be obtained with the typical peak at 1958 cm^{-1} from each fraction. The appropriate target fractions could be obtained from through the SERS map reconstructed from the alkyne Raman peak. The electrospray mass spectrometry (ESI-MS) measurement was performed without silver nanoparticles, indicating the identified Alt-AOMK labeled peptides contained the same sequence, DQGSCGSCWAFGA-VEAISDR with different cleavage sites. To explore the applicability of ATRaS in complex proteolytic mixtures, the test was then performed in HL-60 cell lysate containing CatB. According to the reported results, ATRaS has the great potential to be powerful tool for large-scale screening of targeted molecules in proteomics and chemical biology.

Valuable biomarkers on the surface of tumor cells can help to differentiate the cancer phenotypes, which is of great significance for effective cancer diagnosis and therapy. The normal confocal laser scanning microcopy and flow cytometry have been widely employed for the measurement of surface acceptors on cells based on the fluorescent labels in clinical applications [35–37]. However, these traditional approaches need to collect a large number of cells for the analysis, which are time-consuming and suffer from the photobleaching and interference of background fluorescent signals. To overcome these limitations, Wang *et al.* designed three bioorthogonal SERS nanoprobes labeled with alkyne, azide and nitrile groups for simultaneous targeting and discrimination of multiple breast cancer phenotypes in mice models. The surface of Raman reporter-labeled gold nanoflowers (AuNFs) was encapsulated by silica and polyethylene glycol (PEG) for improving stability and further bioconjugation. To obtain the multiplex targeting SERS nanoprobes, as shown in Fig. 2c, three specific ligands were separately conjugated with nanoparticles: oligonucleotide aptamer (AS1411) targeting nucleolin, cyclic arginine-glycine-aspartic acid (cRGD) peptide for integrin $\alpha_v\beta_3$ and cell adhesion molecule antibody (anti-CD44). These SERS probes manifested extremely low cytotoxicity. To verify the multiplex test, MDA-MB-231 and MCF-7 were selected as cancer cell models. The simultaneous detection of multiplex breast cancer cell phenotypes could be realized by SERS imaging, thereby analyzing the discrimination between MDA-MB-231 cells (overexpressing nucleolin, integrin $\alpha_v\beta_3$ and CD44) and MCF-7 cells (overexpressing nucleolin, integrin $\alpha_v\beta_3$) [38]. Furthermore, the typical Raman peaks of 2205, 2120, and 2230 cm^{-1} could be clearly observed upon carrying out *in vivo* imaging, indicating the presence of the three receptors of nucleolin, integrin $\alpha_v\beta_3$. The bioorthogonal SERS imaging offers an insightful strategy for early discrimination of cancer phenotypes and diagnosis *in vivo* with high sensitivity.

In the process of studying cells, a real-time imaging strategy of biomolecules with high specificity, sensitivity and minimal perturbation is needed [39]. Currently, live cell fluorescence imaging based on fluorophore-labeled biomolecules has been widely applied in biological and biomedical research, while the normal functions of the labeled components may be interfered by the fluorophore [40]. SERS imaging can avoid some interference towards cell function. A new SERS-based bioorthogonal imaging method was developed to visualize cell surface molecules (Fig. 2d). The AuNPs array and silver nanoisland films were prepared for the enhancement of Raman signals, immobilized on the surface of silicon wafers and glass slides, respectively. The cultured cells were imaged on silicon wafers and glass slides with enhanced nanoparticles, while the bioorthogonal Raman reporter molecules were displayed on the SERS spectrum. Various cell surface biomolecules were observed by SERS microscopy through different Raman reporter molecules, including azides, alkynes and carbon-deuterium bonds [41]. The combination of SERS microscope and bioorthogonal Raman reporter molecules expand the function of live cell microscopic imaging and can be used as a supplement to live cell fluorescence imaging and label-free imaging.

The traditional Raman reporter molecules (crystal violet, indocyanine green, rhodamine 6G, cyanine *etc.*) suffer from the complicated Raman signatures, overlap even interference originating from the cellular surrounding components including protein, peptides, and cytochrome c [42,43]. The bioorthogonal Raman reporters without background signals in biological samples attract more and more research interests [44]. Wu *et al.* presented, for the first time, four novel aptamers conjugated biorthogonal SERS nanoprobes for tumor imaging. Four biorthogonal Raman reporters were designed and synthesized based L-cysteine skeleton structure containing benzazido, benzalkyne, and 1,4-diphenyl-buta-1,3-diyn-1-yl moieties with the NHS ester, which located at 2010, 2142, and 2209 cm^{-1}. Then, these bioorthogonal Raman reporters were immobilized on the surface of gold nanoflowers acting as both signal generators and stabilizer. AS1411 (GGT GGT GGT GGT TGT GGT GGT GGT GG) was selected as target unit for specific binding to nucleolin, which highly overexpressed in most of tumor cells while very low levels in normal cells [45,46]. The specific identification of MCF-7 cells and tumor tissue imaging could be achieved utilizing the proposed SERS probes.

Enzyme linked immunosorbent assay (ELISA) has been broadly applied in the field of clinical medicine due to its easy use and relative high sensitivity. However, natural enzymes still suffer from the low stability under severe conditions and high cost for use, which seriously limit the application of ELISA [47,48]. To overcome the limitation of natural enzymes, a SERS immunoassay based on plasmonic $Cu_{2-x}S_ySe_{1-y}$ nanoparticles was fabricated for highly sensitive and selective detection of prostate-specific antigen (PSA) as an important biomarker of prostate cancer, which showed good linear concentration range of 3−120 ng/mL. The $Cu_{2-x}S_ySe_{1-y}$ NPs labeled on the antibodies could efficiently catalyze the click reaction between SERS signal reporter $C{\equiv}C\text{-}PEG_2{-}CH_2CH_2NH_2$ and $N_3\text{-}PEG_3{-}CH_2CH_2NH_2$. Upon the presence of different concentrations of PSA, the sandwich immunocomplex could be obtained. As the click reaction proceeded, the Raman signal of $C{\equiv}C\text{-}PEG_2{-}CH_2CH_2NH_2$ decreased and exhibited a good quantitative relationship with the PSA concentration, which provided a potential platform for the detection of biomarkers in the clinical diagnosis.

3.2. Nucleic acid

Nucleic acids play key important roles in biological heredity, as well as significant biomarkers to monitor the presence and stages in clinical diagnosis. SERS-based technology has been widely applied in nucleic acid detection for the diseases diagnosis [49–51]. The common sensing mechanism is based the hybridization between SERS nanoprobes and target sequences, bring the distance change between SERS nanoprobes and platforms, and SERS signal intensity change [52,53].

Unfortunately, there also have been several challenges for *in vivo* detection of nucleic acids using SERS-based assays: (1) Relative bulky nanostructures of SERS nanoprobes may disturb the normal function and biological process in living cells; (2) SERS nanoprobes cannot be totally accumulated on the interested regions. Therefore, developing new methods for accurate SERS detection of nucleic acids in living cells is still in urgent demand. EdU (5-ethynyl-2′-deoxyuridine) has been presented to readily

incorporate into cellular DNA and accumulate in the nucleus, which can incorporate with alkyne tag to fabricate bioorthogonal SERS tag [54]. As illustrated in Fig. 3a, Yamakosh reported the first alkyne-tagged cell proliferation SERS probe for direct imaging in living cells [55]. Furthermore, Zhang *et al.* adopted EdU as an interior label to precisely locate nuclear region. As a powerful strategy, EdU was introduced into breast cancer cells to improve the content of EdU molecules to obtain the bioinformation of DNA replication process. Then, SERS-based nuclear-targeting nanoprobes incubated with cells to improve Raman sensitivity [56]. The direct SERS imaging of cell nucleus could be obtained, which was different from previous studies that used alkyne as SERS labeling or SERS probes for indirect SERS determination [57].

MicroRNAs (miRNAs) are small non-coding RNA that function in RNA silencing and regulation of gene expression, containing about 22 nucleotides. Furthermore, the abnormal level of miRNAs is closely related to the development of the cancers, and its expression is quite different in various tumors, thus, it can be considered as potential biomarkers for the tumor's detection. At present, the detection of tumor miRNA is still challenging due to its ultralow concentration and complexity, which limits its application in clinical diagnosis [58]. Due to the tumor heterogeneity, the use of one kind of miRNA as the biomarker for the detection is insufficient and cannot meet the clinical specific demand. As shown in Fig. 3b, a new SERS-based sensor array based on the DNA hydrogel was presented to detect nine miRNAs in one sample for the cancer diagnosis, which was fabricated through incorporating a certain multi-component nucleic acid enzymes (MNAzymes) with a DNA hydrogel. At the presence of target miRNAs, DNA hydrogels of the corresponding sensor unit were distinguished accordingly, and SERS tags were able to pass through the hydrogel to be captured by the detection surface, inducing enhanced SERS signals of target miRNA [59]. This integrated platform has great potential for clinical diagnosis of miRNA marked cancer.

3.3. Detection-other reactive species

Glycans have critical roles and participate in various physiological processes in the mantance of cell or tissue structure, cell-cell communication, signal translation and host-pathogen interactions [60,61]. Unfortunately, visualizing glycans on living cells is still challenging due to the nongenetically encoded nature of glycosylation. In order to directly detect unnatural sugars, the alkyne group was introduced to fabricate a bioorthogonal SERS Raman reporter for detection of sialylated glycans. The peracetylated *N*-(4-pentynoyl) mannosamine (Ac4ManNAl) could be converted to the sialic acids (SiaNA1) after incubation with cells, which exhibited characterized alkyne peak of at 2120 cm^{-1} for Ac4ManNA1 and 2113 cm^{-1} for SiaNA1, respectively. The gold nanoparticles with diameter of about 120 nm were prepared as the active SERS substrate, which were functionalized with 4-mercaptophenylboronic acid (MPBA) to improve the identification of the sialylated glycans. As a result, the characterized alkyne peak of SiaNA1 in SERS spectra was obtained at about 2121 cm^{-1} on the MPBA-AuNP substrate, while no peak observed within the silent region for natural sialic acid [62]. The proposed bioorthogonal SERS strategy showed high sensitivity and specificity to the glycans.

Carbon monoxide (CO) is recognized as the essential gas signaling small molecule participating in various physiological processes. Despite its importance, detection of CO in biological systems is still challenging due to the lack of efficient detection or visualization tool [63]. Currently, the major assay for CO focuses on the fluorescent probe of organopalladium. However, these

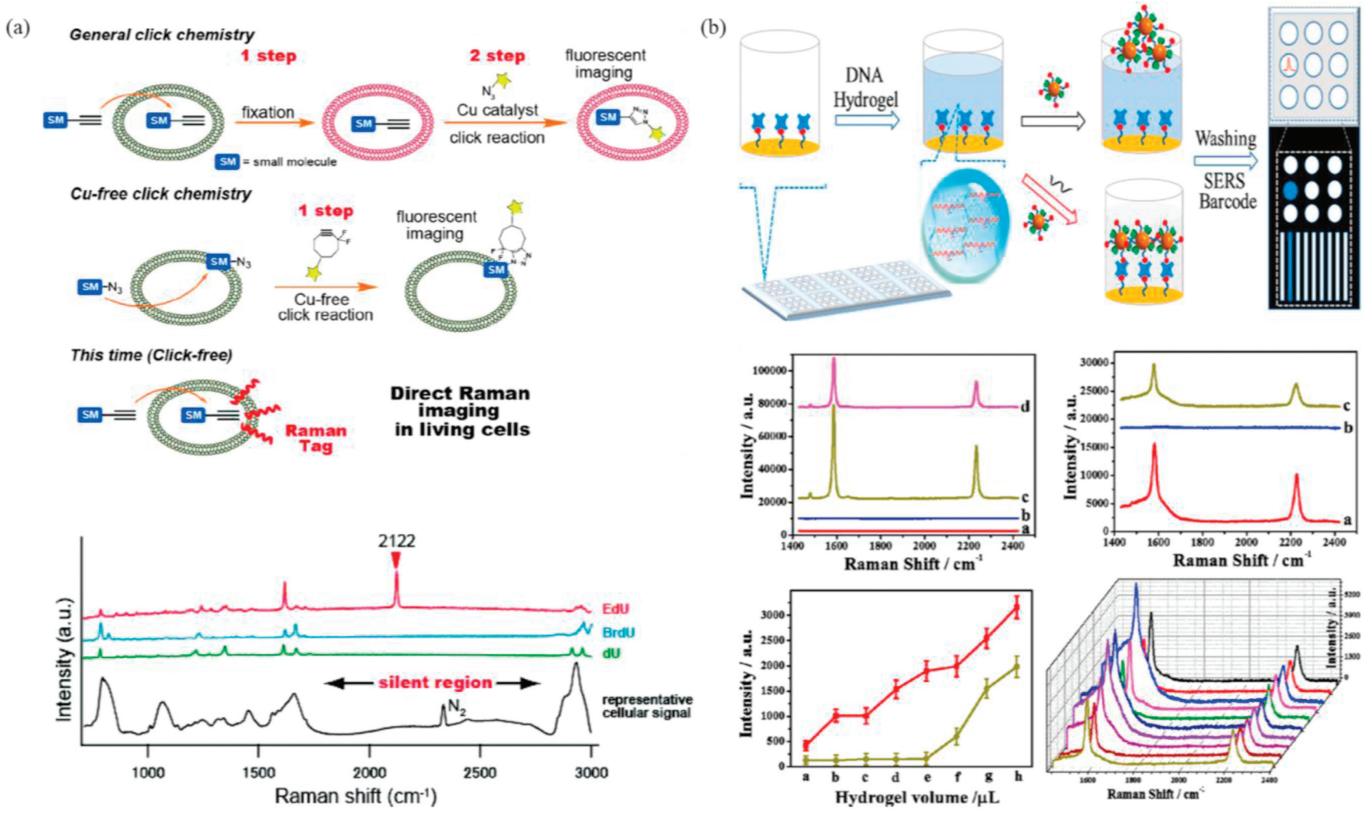

Fig. 3. (a) Concept of click-free imaging and structures of thymidine analogues. Copied with permission [55]. Copyright 2011, American Chemical Society; (b) Schematic illustration of the preparation and application of the target miRNA-responsive DNA hydrogel-based SERS sensor array for measuring multiple miRNAs in one sample. Copied with permission [59]. Copyright 2020, American Chemical Society.

molecular fluorescent probes may be interfered by different pH values in various organelles. Qin *et al.* reported a SERS nanoprobe for detection of CO based on the ruthenium(II)-vinyl displacement reaction, as shown in Fig. 4a. The gold-silver alloy nanoparticle was selected as the active substrate, and then an alkyne/ruthenium(II) ligand immobilized on the surface of the substrate for recognition of CO. To improve the chemical stability of SERS probe, a porous silica shell was introduced. Upon addition of CO, the alkyne ligand was displaced resulting in the decrease of the alkyne vibration (~2206 cm^{-1}), and the increase of metal carbonyl complex (~2100 cm^{-1}), which allowed to ratiometric analysis of the CO levels [64].

Reactive oxygen species (ROS) are indispensable in regulating cell signaling, homeostasis and other biological processes. The excessive amount of ROS will induce the cellular oxidative stress and interrupt the dysfunction of protein, DNA and other biomolecules, even result in the cell death [65]. This unique property of ROS can be utilized to efficiently damage and kill cancer cell to realize the excellent therapeutic outcome with the assistance of drugs. As one of major ROS, hydrogen peroxide (H_2O_2) plays vital important roles serving as signaling molecule in various biological processes. The current H_2O_2 detection methods mainly focus on colorimetric assay, electrochemical method and fluorescence analysis. Unfortunately, even the commonly utilized fluorescence analysis still suffers from unavoidable shortcoming, such as rapid photobleaching and the interference from other intracellular components. Inspired by the reaction of H_2O_2 and borate moiety, a new kind of Au-Ag alloy substrate with silica encapsulation (AuAg@p-SiO_2) was prepared to develop the alkyne-based SERS nanoprobe for the analysis of H_2O_2 in living cells

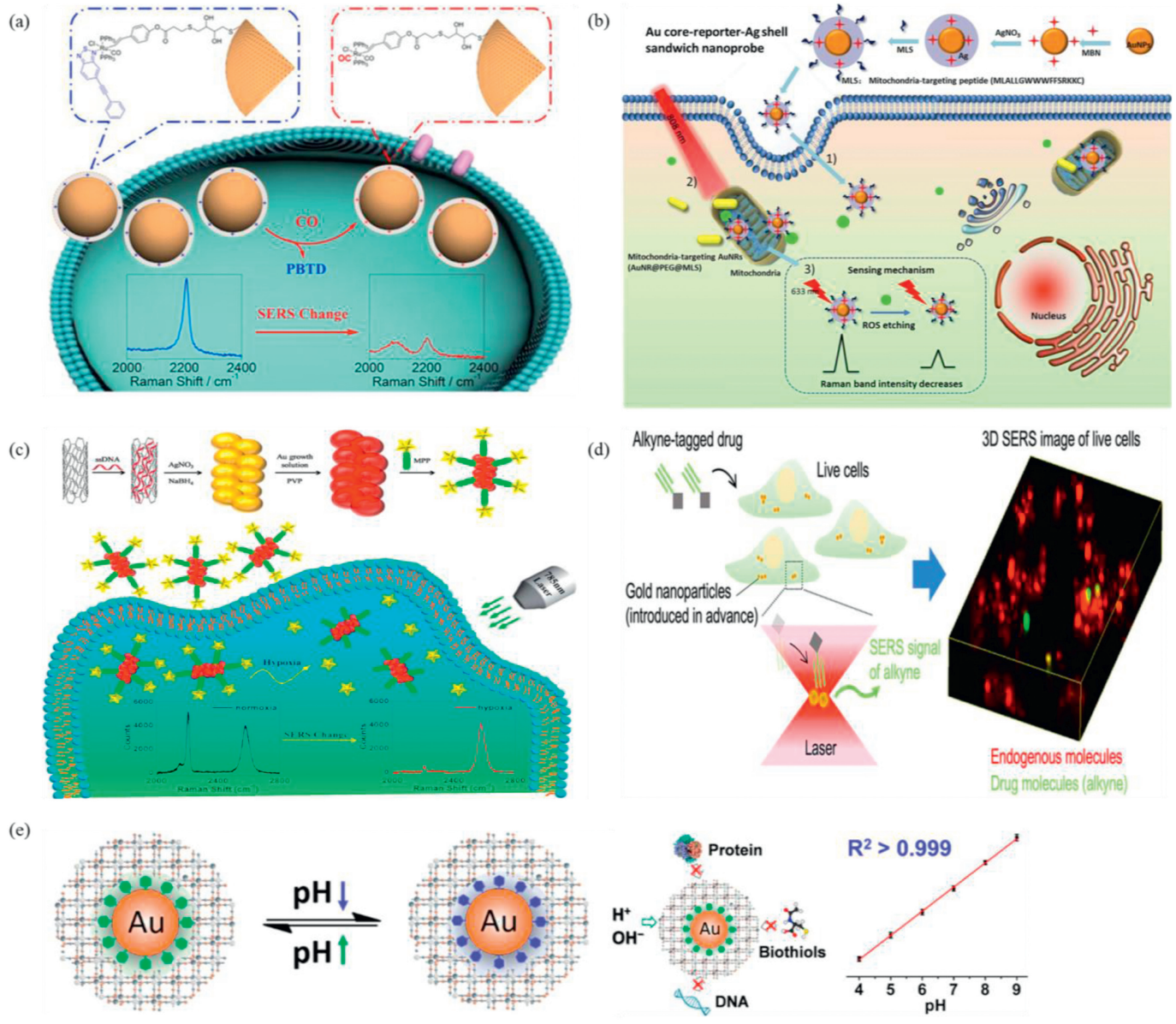

Fig. 4. (a) Synthetic scheme for the alkyne/ruthenium(II) complex, and schematic illustration of the preparation of the SERS nanoprobe and its sensing mechanism. Copied with permission [64]. Copyright 2019, American Chemical Society; (b) Schematic illustration of the AuAg@p-SiO_2NPs-based SERS nanosensor for alkyne-mediated ratiometric Raman detection of H_2O_2. Copied with permission [66]. Copyright 2019, Elsevier; (c) The preparation of the SWCNT/Ag/AuNPs/MPP conjugate-based SERS nanoprobe and the sensing mechanism of hypoxia. Copied with permission [69]. Copyright 2019, American Chemical Society; (d) Schematic diagram of SERS nanoprobe detection principle and concept of click-free imaging and structures of thymidine analogues. Copied with permission [71]. Copyright 2020, American Chemical Society; (e) Working principle, and pH responses of the PB-caged SERS probe. Copied with permission [75]. Copyright 2020, American Chemical Society.

(Fig. 4b) [66]. The AuAg NPs were functionalized with 4-mercaptophenylboronic acid (MPBA) and 4-mercaptophenlyacetylene (MPAE) as an internal standard, and then dopamine (DA) was introduced to improve the uniformity. The ratiometric SERS nanoprobe was fabricated *via* the amide bond between the amino group of DA and the carboxyl group of 3-(4-(phenylethynyl) benzylthio) propanoic acid (PEB, 2214 cm^{-1}). Upon treatment of H_2O_2, the SERS signal at 2214 cm^{-1} remarkably decreased since the boronate-to-phenol switch induced the release of the alkynyl on the PEB from the surface of SERS nanoprobe. The quantitative analysis could be realized based on the ratiometric values of I_{1986}/I_{2214} because of the changeless of SERS signal of MAPE at 1986 cm^{-1}. Under the optimized conditions, the limit of detection was calculated to be as low as 52 nm, which provided a new detection approach for measurement of H_2O_2 by using different signaling agents.

3.4. Biological and physiological processes

Hypoxia is one of the characteristics of various diseases, which can be served as an important indicator to demonstrate the progression of diseases [67,68]. Currently, several powerful techniques have been developed to achieve the detection of hypoxic region, such as immunostaining positron emission tomography (PET), magnetic resonance imaging (MRI), phosphorescence, and fluorescence imaging. However, phosphorescence imaging and immunostaining require long time and harsh conditions. Fluorescence imaging with high sensitivity and selectivity usually suffers from the interference of environmental conditions. SERS becomes a new choice to develop powerful tools for hypoxic imaging due to low autofluorescence, resistance to photobleaching, low phototoxicity, and excellent multiple detection capability. To overcome these limitations, a ratiometric SERS nanoprobe based on azo-alkynes as Raman reporters was constructed for imaging living cells and tissues under hypoxic conditions in cellular silent region, which comprised Ag/Au alloy nanoparticles and single-walled carbon nanotube (SWCNT/Ag/AuNPs) (Fig. 4c) [69]. The Ag/Au alloy produced high SERS enhancement, low cytotoxicity and excellent chemical stability. The SWCNT provided sharp scattering peaks at their 2D-band (~2578 cm^{-1}), while the Raman reporter exhibited typical peak (2207 cm^{-1}). Under hypoxic condition, the Raman reporter molecules were reduced by reductases and left from the SERS probes, inducing the decrease of alkyne Raman intensity at 2207 cm^{-1}. The ratiometric detection of hypoxia level could be achieved *via* the ratio of two peak intensities (I_{2578}/I_{2207}) in HepG2 and HeLa living cells and rat liver tissue, indicating the ratiometric SERS probe may be powerful tool in the hypoxia research and clinical applications.

Raman microscopy as a noninvasive detection technology is widely applied in the field of biomedicine. In the absence of markers, the distribution of visual molecules can be observed using Raman microscopy [70]. Visualizing uptake of drugs plays key vital role for drug development and pharmaceutical science. However, the Raman peaks of interest drug molecules are interfered by numerous endogenous molecules, exhibiting strong Raman peaks. To differentiate the specific Raman signals from the background signals, alkyne moiety as powerful Raman-tag has been proposed and applied in the biomedical research. Combining the high sensitivity of SERS detection, an alkyne-based SERS three-dimensional (3D) imaging method was proposed to real-time monitor the drug uptake and track the drug distribution with high temporal resolution in live cells (Fig. 4d) [71,72]. The alkyne-tagged acyloxymethyl ketone type inhibitor (Alt-AOMK), was selected as small-molecule drug model. AuNPs were incubated and entered into lysosomes of living cells through endocytosis to reflect the arrival of alkyne-tagged drugs. The enhanced Raman signal of alkyne could be obtained due to the high affinity of terminal alkynes to the surface of AuNPs when alkyne-tagged drugs were colocalized with the AuNPs. Upon utilizing time-lapse 3D SERS imaging, the drug uptake by live cells could be investigated in different chemical conditions and biological models such as H9c2 cells, NIH-3T3 and MCF-7 cells. Furthermore, the quantitative analysis was performed using dital SERS counting to statistically visualize the relative change of drug concentrations and the dynamic process of drug uptake. The combined strategy between alkyne-tag and SERS technique has a great potential to be potential bioorthogonal imaging to real-time visualize the drug uptake in live cells for pharmaceutical research.

3.5. pH

Normal physiological functions require pH homeostasis, whether in the cell (pH_i) or outside the cell (pH_e), which plays important roles in many physiological processes including protein synthesis, physiological function regulation and cell communications [73]. However, the imbalance of pH may also lead to disease and cancer. At present, small molecule probes for detecting pHi are commonly used and effective tools in chemical biology, helping to study the important role of pH in cell functions and diseases. However, fluorescent probes still have shortcomings when detecting pH_i. To overcome these limitations, a series of low molecular weight (< 260) detection strategies for oligoyne compounds were developed, and the ratio pH_i was determined by Raman microscopy [74]. Since these compounds exhibited Raman spectroscopy that ere sensitive to pH, the p*K*a (H) values of these compounds were adjusted to achieve physiologically relevant pH sensitivity for monitoring pH changes. The intracellular pH sensitivity test proved that compound 13 could be applied to detect the pH_i in PC3 cells proportionally and monitor the pH_i changes of steady-state inhibitors. This alkyne tag Raman imaging (ATRI) accurately determines pH through Raman microscopy, and its unique properties make it a new strategy complementary to fluorescent probes.

Intracellular pH is closely related to various physiological processes. Abnormal pH in cells can lead to abnormal organelles and cell functions, which may lead to diseases and cancer. Current methods for measuring pH changes include microelectrodes, nuclear magnetic resonance, UV–vis absorption spectroscopy, fluorescence spectroscopy, and SERS spectroscopy. SERS technology has been widely applied to the field of biomedicine to detect intracellular biomarkers. However, SERS technology still has some limitations. For example, intracellular substances may interfere with the SERS probe, leading to inaccurate measurement results, and the complex cytoplasmic environment greatly weakens the colloidal stability of the SERS probe. In order to overcome these limitations, a SERS probe based on Prussian blue (PB) pH response was designed and synthesized to quantify dynamic pH changes in living cells (Fig. 4e). The pH responsive Raman reporter (4-MPY) was directly anchored on the AuNP surface [75,76]. The PB shell acted as a protective layer to directly wrap the SERS probe. The PB shell with sub-nanometer scale porous structure allowed the entry of only small biological molecules rather than biological macromolecules by reacting with the SERS probe. The nitrile (C≡N) in PB was used as a reference in the Raman-silent region and compared with the Raman signal that varies with the pH concentration. By monitoring the dynamic pH changes during autophagy, it was proved that the SERS probe could reliably quantify subtle pH changes in living cells. This highly reliable and accurate SERS probe might also be suitable for understanding the relationship between normal cell physiological processes and pH.

4. Phototherapy

In recent decades, a large number of treatment strategies have been developed and utilized as effective treatment tools to improve the treatment effect, including photothermal therapy (PTT), photodynamic therapy (PDT), gene therapy, chemotherapy, and immunotherapy. Among them, PTT and PDT have attracted increasing attention due to the high therapeutic efficiency, noninvasiveness, excellent targeting, and minimal side effects [77].

PTT can convert near infrared (NIR) into heat, thereby increasing the temperature of the tumor and effectively killing cancer cells with minimal effect to healthy cells and tissues. SERS imaging in the Raman silent region is combined with PTT to perform highly sensitive SERS detection [78]. Furthermore, the NIR laser can be converted to high temperature to kill cancer cells. And the time and intensity of irradiation laser can be controlled accurately and flexibly, photothermal ablation has outstanding advantages in fixed-point operation, significant therapeutic effect, specificity and safety [79]. Here, photosensitizers (PSs) absorb the light energy and transfer excited electrons to produce radical anion species or directly lead triplet oxygen to generate singlet oxygen, which can kill cancer cells with noninvasiveness and high selectivity.

Accurate diagnosis and effective therapy of breast cancer are essential to improve the survival rate of patients. Conventional cancer detection in clinical medicine still has limitations. For example, X-ray computed tomography (CT) and magnetic resonance imaging (MRI) have low sensitivity and low specificity, and positron emission tomography (PET) combined with CT is expensive and radioactive [80]. Therefore, the SERS diagnosis and treatment platform was developed to achieve *in situ* noninvasive cancer precise detection and treatment [81]. Herein, a bioorthogonal SERS probe was prepared for precise diagnosis and effective therapy of cancer (Fig. 5a). Designed and synthesized lipoic acid conjugated bioorthogonal Raman reporters, and then directly anchored on the surface of gold nanorods (AuNRs), AuNRs showed enhanced Raman signal at 2205 cm^{-1}. Two aptamers (AS1411 or MUC1) were selected to anchor on the surface of AuNR to specifically identify nuclelin and mucin-1 proteins overexpressed in cancer cells. Because AuNR has high photothermal conversion efficiency, when SERS nanotags are intravenously injected into mice, SERS nanotags can cause cancer cell poisoning. Experimental studies *in vitro* and *in vivo* have proved that SERS nanotags have a 99% inhibition rate of cancer after laser irradiation, and they have good biocompatibility. In this study, SERS nanotags can be applied as a precise therapeutic diagnostic platform for cancer diagnosis and photothermal therapy.

Recently, various functional materials have been developed as photothermal transduction agents (PTAs) for efficient photothermal therapy such as organic molecules, metal nanomaterials, carbon-based nanomaterials, and conjugated polymers. Unfortunately, many PTAs can directly convert the light energy into heat, inducing the unavoidable thermal damage to the surrounding heathy tissues [82]. Although several strategies have been developed to reduce the damage to healthy tissues through introduction of pathogen specific targeting groups including antibodies, polymers, side effects cannot be completely prevented [83,84]. There is an urgent need to develop more specific strategies of PTAs to reduce the thermal damage to cells and improve the therapy efficiency. To meet the urgent demand, Jiang *et al.* presented a new strategy based on bacteria-induced gold nanoparticles (AuNPs) *in situ* aggregation on the bacteria surface through specific targeting of vancomycin and bioorthogonal cycloaddition (Fig. 5b). The aggregated AuNPs not only provided efficient SERS imaging of bacteria due to the 'hot spot' effect located in adjacent AuNPs, but also exhibited excellent photothermal conversion efficiency, allowing enhanced photothermal killing bacteria. Fortunately, in the absence of bacteria, the AuNPs could keep dispersible stably and display no damage to normal tissues. This powerful strategy exhibited great potential for photothermal elimination of bacteria integrating SERS imaging.

Imaging-guided phototherapy can evaluate the therapy outcome as well as improve the therapy precision due to visualization of transportation and distribution of the agents. Multimodal imaging-guided phototherapy, such as SERS imaging and magnetic resonance imaging (MRI), provides great opportunities in cancer diagnosis. Owing to their individual advantages, numerous efforts have been devoted to fabricating the integrated platform of PTT and PDT to realize better therapeutic outcomes [85]. Shen and coworkers presented monodispersed Prussian blue-encapsulated gold nanoparticles (Au@PB NPs) for both MRI and SERS imaging due to the introduction coordination polymer containing cyanide and iron ions [86,87]. PB can be easily assembled onto the surface of AuNPs and utilized as source of MRI and SERS. More importantly, PB can efficiently the NIR light energy and be used as photosensitizer for PTT and PDT simultaneously. In addition, to improve the effective concentration of the therapy agent in cancer cells, hyaluronic acid (HA) was selected as targeting moiety due to the

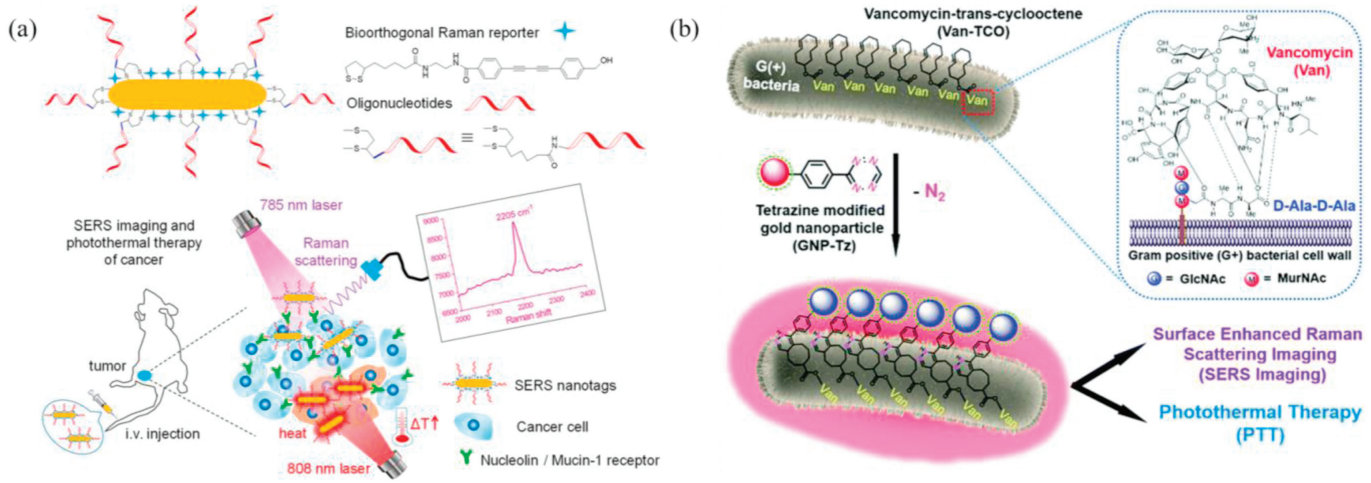

Fig. 5. (a) Fabrication of oligonucleotide modified bioorthogonal SERS nanotags. Copied with permission [81]. Copyright 2020, American Chemical Society; (b) Scheme diagram of bacteria-induced gold nanoparticle aggregation for SERS imaging and enhanced photothermal ablation of Gram-positive bacteria. Copied with permission [82]. Copyright 2019, the Royal Society of Chemistry.

overexpression of HA specific receptors (*e.g.*, CD44), which exhibited more accumulation in cancer cells. The integration of SERS/MR imaging-guided phototherapy by Au@PB@HA provides excellent opportunity for diagnosis and therapy in cancer treatment.

5. Conclusion and perspective

In the previous decade, many significant advances and technique development have been obtained in the field of bioorthogonal SERS imaging, which attracts much attention for living-cell imaging and whole-tissue studies. The most attractive feature is that the bioorthogonal Raman molecules can directly label the targets as well as ignore the impact on normal physiological activities, which makes the *in situ* and real-time visualization possible. In contrast, the common fluorophore or nanoparticle or enzyme is often too big in size to be metabolized, and usually interferes the normal physiological functions and processes, which limits their application in biological and biomedical research. Since SERS technique exhibits high sensitivity, multiple-detection capability, and resistance to photobleaching, the integration of SERS detection and bioorthogonal label will be an excellent strategy for visualization of living cells and tissues, even for the disease diagnosis.

It is worth noting that SERS stable labeling might alter the normal chemical and physiological properties of the substrate, even it has great potential in biomedicine, cell biology and environmental microbiology. Thus, the application of this strategy should be used with caution. Cell imaging can be expanded by integrating the types of bioorthogonal SERS tags into biomolecules through triple bond functional groups. This strategy not only has the labeling ability that does not interfere with the chemical properties of the substrate, but also has the properties of multiplexing imaging beyond traditional fluorescence imaging, which will make expected contribution for biological imaging. Although further improvement is desired for this strategy, the methodological development and biological and biomedical application have already demonstrated the potential in future research. We expect that bioorthogonal SERS imaging holds the prospect to monitor the specific cellular functions as the complement.

Declaration of competing interest

The authors declare that they have no known competing financial interests or personal relationships that could have appeared to influence the work reported in this paper.

Acknowledgments

This work was supported by Hainan Provincial Natural Science Foundation of China (Nos. 2019RC220, 820RC641, 2019RC210), National Natural Science Foundation of China (Nos. 21864011, 22064009, 21775162), Hainan Key Research and Development Project (No. ZDYF2020133), CAMS Innovation Fund for Medical Sciences (No. 2019-I2M-5-023), Nanhai Young-Talent Program of Hainan (No. 20202007), and Hundred Talent Program of Hainan (2018).

References

[1] J. Langer, D. Jimenez de Aberasturi, J. Aizpurua, et al., ACS Nano 14 (2020) 28–117.
[2] D. Cialla-May, X.S. Zheng, K. Weber, J. Popp, Chem. Soc. Rev. 46 (2017) 3945–3961.
[3] C. Zong, M. Xu, L.J. Xu, et al., Chem. Rev. 118 (2018) 4946–4980.
[4] X. Liu, X. Liu, P. Rong, D. Liu, Trends Analyt. Chem. 123 (2020) 115765.
[5] Y. Zeng, K.M. Koo, M. Trau, A.G. Shen, J.M. Hu, Appl. Mater. Today 15 (2019) 431–444.
[6] S. Laing, L.E. Jamieson, K. Faulds, D. Graham, Nat. Rev. Chem. 1 (2017) 1–19.
[7] Y. Wang, B. Yan, L. Chen, Chem. Rev. 113 (2013) 1391–1428.
[8] K. Kneipp, H. Kneipp, I. Itzkan, R.R. Dasari, M.S. Feld, Chem. Rev. 99 (1999) 2957–2976.
[9] A. Campion, P. Kambhampati, Chem. Soc. Rev. 27 (1998) 241–250.
[10] E. Saxon, C.R. Bertozzi, Science 287 (2000) 2007–2010.
[11] H.C. Kolb, M.G. Finn, K.B. Sharpless, Angew. Chem. Int. Ed. 40 (2001) 2004–2021.
[12] S.L. Scinto, O. Ekanayake, U. Seneviratne, et al., J. Am. Chem. Soc. 141 (2019) 10932–10937.
[13] Kenry, B. Liu, Trends Chem. 1 (2019) 763–778.
[14] H.W. Shih, D.N. Kamber, J.A. Prescher, Curr. Opin. Chem. Biol. 21 (2014) 103–111.
[15] S. Hong, L. Lin, M. Xiao, X. Chen, Curr. Opin. Chem. Biol. 24 (2015) 91–96.
[16] W.R. Algar, D.E. Prasuhn, M.H. Stewart, et al., Bioconjug. Chem. 22 (2011) 825–858.
[17] R. Xie, S. Hong, X. Chen, Curr. Opin. Chem. Biol. 17 (2013) 747–752.
[18] G. Yi, J. Son, J. Yoo, C. Park, H. Koo, Biomaterials Res. 22 (2018) 1–8.
[19] Y. Li, Z. Wang, X. Mu, A. Ma, S. Guo, Biotechnol. Adv. 35 (2017) 168–177.
[20] J. Wardle, K. Robb, S. Vernon, J. Waller, Am. Psychol. 70 (2015) 119–133.
[21] J.F. Li, Y.J. Zhang, S.Y. Ding, R. Panneerselvam, Z.Q. Tian, Chem. Rev. 117 (2017) 5002–5069.
[22] L.A. Lane, X. Qian, S. Nie, Chem. Rev. 115 (2015) 10489–10529.
[23] J. Kneipp, ACS Nano 11 (2017) 1136–1141.
[24] Z.L. Song, X.H. Zhao, W.N. Liu, et al., Small 9 (2013) 951–957.
[25] Z.L. Song, Z. Chen, X. Bian, et al., J. Am. Chem. Soc. 136 (2014) 13558–13561.
[26] S. Li, T. Chen, Y. Wang, et al., Angew. Chem. Int. Ed. 56 (2017) 13455–13458.
[27] S. Lee, H. Chon, J. Lee, et al., Biosens. Bioelectron. 51 (2014) 238–243.
[28] Y. Lyu, Y. Fang, Q. Miao, et al., ACS Nano 10 (2016) 4472–4481.
[29] M. Li, J. Wu, M. Ma, et al., Nanotheranostics 3 (2019) 113–119.
[30] K. Lang, J.W. Chin, Chem. Rev. 114 (2014) 4764–4806.
[31] T. Peng, X. Yuan, H.C. Hang, Curr. Opin. Chem. Biol. 21 (2014) 144–153.
[32] A. Deiters, T.A. Cropp, M. Mukherji, et al., J. Am. Chem. Soc. 125 (2003) 11782–11783.
[33] J. Ando, M. Asanuma, K. Dodo, et al., J. Am. Chem. Soc. 138 (2016) 13901–13910.
[34] J. Szychowski, A. Mahdavi, J.J.L. Hodas, et al., J. Am. Chem. Soc. 132 (2010) 18351–18360.
[35] A.N. Ramya, M.M. Joseph, J.B. Nair, et al., ACS Appl. Mater. Interfaces 8 (2016) 10220–10225.
[36] J.W. Kang, P.T.C. So, R.R. Dasari, D.K. Lim, Nano Lett. 15 (2015) 1766–1772.
[37] A. Oseledchyk, C. Andreou, M.A. Wall, M.F. Kircher, ACS Nano 11 (2017) 1488–1497.
[38] J. Wang, D. Liang, J. Feng, X. Tang, Anal. Chem. 91 (2019) 11045–11054.
[39] T.Y. Liu, K.T. Tsai, H.H. Wang, et al., Nat. Commun. 2 (2011) 538.
[40] L. Wei, F. Hu, Y. Shen, et al., Nat. Methods 11 (2014) 410–412.
[41] M. Xiao, L. Lin, Z. Li, et al., Chem. Asian J. 9 (2014) 2040–2044.
[42] X. Jiang, Z. Jiang, T. Xu, et al., Anal. Chem. 85 (2013) 2809–2816.
[43] S. Lee, S. Kim, J. Choo, et al., Anal. Chem. 79 (2007) 916–922.
[44] H. An, B. Jin, Biotechnol. Adv. 30 (2012) 1721–1732.
[45] J. Wu, D. Liang, Q. Jin, et al., Chem. Eur. J. 21 (2015) 12914–12918.
[46] L. Li, J. Hou, X. Liu, et al., Biomaterials 35 (2014) 3840–3850.
[47] L. Yang, M.X. Gao, H.Y. Zou, Y.F. Li, C.Z. Huang, Anal. Chem. 90 (2018) 11728–11733.
[48] Y. Yin, Q. Li, S. Ma, et al., Anal. Chem. 89 (2017) 1551–1557.
[49] E. Garcia-Rico, R.A. Alvarez-Puebla, L. Guerrini, Chem. Soc. Rev. 47 (2018) 4909–4923.
[50] J. Su, D. Wang, L. Norbel, et al., Anal. Chem. 89 (2017) 2531–2538.
[51] Z. Wang, S. Zong, L. Wu, D. Zhu, Y. Cui, Chem. Rev. 117 (2017) 7910–7963.
[52] X. Wang, N. Choi, Z. Cheng, et al., Anal. Chem. 89 (2017) 1163–1169.
[53] K. Dardir, H. Wang, B.E. Martin, et al., J. Phys. Chem. C 124 (2020) 3211–3217.
[54] K. Meister, J. Niesel, U. Schatzschneider, et al., Angew. Chem. Int. Ed. 49 (2010) 3310–3312.
[55] H. Yamakoshi, K. Dodo, M. Okada, et al., J. Am. Chem. Soc. 133 (2011) 6102–6105.
[56] A. Huefner, W.L. Kuan, R.A. Barker, S. Mahajan, Nano Lett. 13 (2013) 2463–2470.
[57] J. Zhang, L. Liang, X. Guan, et al., Anal. Bioanal. Chem. 410 (2018) 585–594.
[58] C.P. Liang, P.Q. Ma, H. Liu, et al., Angew. Chem. Int. Ed. 56 (2017) 9077–9081.
[59] Y. Si, L. Xu, N. Wang, et al., Anal. Chem. 92 (2020) 2649–2655.
[60] R. Xie, S. Hong, L. Feng, J. Rong, X. Chen, J. Am. Chem. Soc. 134 (2012) 9914–9917.
[61] S. Ye, E. Zaitseva, G. Caltabiano, et al., Nature 464 (2010) 1386–1389.
[62] L. Lin, X. Tian, S. Hong, et al., Angew. Chem. Int. Ed. 52 (2013) 7266–7271.
[63] Y. Cao, D.W. Li, L.J. Zhao, et al., Anal. Chem. 87 (2015) 9696–9701.
[64] X. Qin, Y. Si, Z. Wu, et al., Anal. Chem. 92 (2020) 924–931.
[65] Y. Wen, F. Huo, C. Yin, Chin. Chem. Lett. 30 (2019) 1834–1842.
[66] Y. Si, L. Li, X. Qin, et al., Anal. Chim. Acta 1057 (2019) 1–10.
[67] X. Zheng, X. Wang, H. Mao, et al., Nat. Commun. 6 (2015) 5834.
[68] J.N. Liu, W. Bu, J. Shi, Chem. Rev. 117 (2017) 6160–6224.
[69] X. Qin, Y. Si, D. Wang, et al., Anal. Chem. 91 (2019) 4529–4536.
[70] H. Yamakoshi, A. Palonpon, K. Dodo, et al., Bioorg. Med. Chem. Let. 25 (2015) 664–667.
[71] K. Koike, K. Bando, J. Ando, et al., ACS Nano 14 (2020) 15032–15041.
[72] K. Sepp, M. Lee, M.T.J. Bluntzer, et al., J. Med. Chem. 63 (2020) 2028–2034.

[73] T. Myochin, K. Kiyose, K. Hanaoka, et al., J. Am. Chem. Soc. 133 (2011) 3401–3409.
[74] L.T. Wilson, W.J. Tipping, L.E. Jamieson, et al., Analyst 145 (2020) 5289–5298.
[75] Y. Bi, H. Di, E. Zeng, et al., Anal. Chem. 92 (2020) 9574–9582.
[76] L.J. Xu, Z.C. Lei, J. Li, et al., J. Am. Chem. Soc. 137 (2015) 5149–5154.
[77] T.T. Xu, J.H. Li, F.R. Cheng, et al., Chin. Chem. Lett. 28 (2017) 1885–1888.
[78] J. Feng, L. Chen, Y. Xia, et al., ACS Biomater. Sci. Eng. 3 (2017) 608–618.
[79] Y. Chen, L. Li, W. Chen, H. Chen, J. Yin, Chin. Chem. Lett. 30 (2019) 1353–1360.
[80] Y. Huang, K. Xia, N. He, et al., Sci. China Chem. 58 (2015) 1759–1765.
[81] Y. Wang, Y. Song, G. Zhu, D. Zhang, X. Liu, Chin. Chem. Lett. 29 (2018) 1685–1688.
[82] H. Wang, W. Ouyang, X. Zhang, et al., J. Mater. Chem. B 7 (2019) 4630–4637.
[83] S. Lee, S. Jung, H. Koo, et al., Biomaterials 148 (2017) 1–15.
[84] H.J. Chung, T. Reiner, G. Budin, C, et al., ACS Nano 5 (2011) 8834–8841.
[85] W. Zhu, M.Y. Gao, Q. Zhu, et al., Nanoscale 12 (2020) 3292–3301.
[86] K. Deng, Z. Hou, X. Deng, et al., Adv. Mater. 25 (2015) 7280–7290.
[87] M.A. Komkova, E.E. Karyakina, A.A. Karyakin, J. Am. Chem. Soc. 140 (2018) 11302–11307.